0152

Motion corrected magnetization transfer-mediated fingerprinting (MT-MRF) using DISORDER.

Daniel J. West[1], Lucilio Cordero-Grande[1,2,3], Rui P. A. G. Teixeira[1,2], Giulio Ferrazzi[4], Joseph V. Hajnal[1,2], and Shaihan J. Malik[1,2]
[1]Biomedical Engineering and Imaging Sciences, King's College London, London, United Kingdom, [2]Centre for the Developing Brain, King's College London, London, United Kingdom, [3]Biomedical Image Technologies, ETSI Telecomunicación, Universidad Politécnica de Madrid & CIBER-BNN, Madrid, Spain, [4]IRCCS San Camilo Hospital, Venice, Italy

Synopsis

ihMT is a promising approach for myelin imaging due to its specificity to substances with non-zero dipolar order. However, tissue model quantification requires high resolution acquisitions in excess of twenty minutes in length and so necessitates the use of motion correction methods to prevent artefacts. In this work we combine our recent MT-mediated MRF sequence with the DISORDER retrospective motion correction method. This new framework can acquire and reconstruct high resolution motion-compensated 3D time-resolved data from fingerprinting sequences. Semi-quantitative MT and ihMT ratio maps as well as quantitative maps of tissue parameters can be obtained from the resulting images.

Introduction

Inhomogeneous magnetization transfer (ihMT) contrast is sensitive to myelin[1,2] and, as we have previously shown, can be generated efficiently using multiband RF pulses either in a steady-state[3] or cyclic-state[4] framework. In the example shown in Figure 1, the sequence alternates between RF pulses with 1, 2 and 3 bands, constructed such that the on-resonance flip angle never changes[5]. Tissues with no significant MT or ihMT effect give constant signal throughout but MT-mediated time-varying signal fluctuations are generated in most brain tissues. When combined with randomized encoding, these time-varying signals are akin to an MRF sequence, and resulting data can be reconstructed using the low-rank inversion (LRI) approach proposed by Assländer *et al.*[6]

However, 3D brain volume acquisitions using these methods can exceed a duration of twenty minutes, so motion correction techniques are required to prevent imaging artefacts. Cordero-Grande *et al.* proposed a motion estimation method whereby partial *k*-space information provided by receiver coils is used to estimate the position of an imaged object during multi-shot acquisitions[7]. This was subsequently combined with randomized-chequered Cartesian trajectories to boost motion resolvability in the so-called DISORDER method[8]. In this work we show that LRI MRF reconstruction and the Cartesian DISORDER motion estimation/compensation framework can be combined for motion-tolerant and well-conditioned reconstructions for our MT-MRF sequence.

Methods

Although joint motion estimation and LRI is conceptually possible, we have observed that for our application it is more efficient to split these subproblems. Motion estimation can be accomplished as in conventional DISORDER. Then, motion corrected MT-MRF datasets can be reconstructed by incorporating a low-rank representation of a dictionary of signal evolutions U_R (computed via SVD and shuffled to match *k*-space collection ordering) and motion operators T_θ (from estimated parameters θ) into a conjugate-gradient sensitivity encoding reconstruction:

$$[1]\ \hat{\mathbf{x}} = \arg\min_{\mathbf{x}} ||\mathbf{U_R F S T_\theta x} - \mathbf{y}||_2^2$$

x are singular values of a low-rank approximation to the temporal signal evolution in each voxel, S are coil sensitivities, F represents a discrete Fourier transform and y is measured *k*-space data.

Experiments were conducted on a 1.5T Philips Ingenia MR system using a bSSFP sequence with parameters: repetition time = 5.3ms, flip angle = 29.5˚, pulse duration = 2ms, off-resonance frequency = 8.1kHz and root-mean-square B_1 = 4μT.

Three phantoms were scanned with FOV = 182×364×240mm (Cartesian sampling): $MnCl_2$-doped water (0.05mM concentration; no MT effect), bovine serum albumin (BSA; MT but no ihMT effect) and prolipid 161 (PL161; strong ihMT effect), resulting in a scan time of 13.5 minutes (5 fully-encoded volumes). Figure 2 illustrates sampling order of the phase-encoding plane.

A healthy adult male volunteer (aged 24) was scanned using the same acquisition scheme as for the phantom experiment but FOV = 200×400×364mm and scan time was ~40 minutes (16 fully-encoded volumes) for a 2mm isotropic resolution to improve SNR. 1200 time-points were reconstructed (Figure 1), making our method highly undersampled. One motion estimate was obtained approximately every twenty seconds - sufficient for the involuntary motion considered here. Equation 1 was used to reconstruct all datasets before time domain volumes at t_1, t_2 and t_3 were combined to produce MT ratio (MTR) and ihMT ratio (ihMTR) maps. Since the signals display temporal evolution, quantification of tissue parameters can be achieved using dictionary fitting. However, the ihMT signal model has nine free parameters that cannot all be estimated so, similar to other studies[9,10], we use a constrained fit but for estimation of free pool T_1^f, semisolid fraction *f* and dipolar T_{1D}^s.

Results

Figure 3 summarizes results from a phantom experiment. MT effects only exist in BSA and PL161, while only PL161 provides a non-negligible ihMTR of ~20%.

Using DISORDER, estimates of translational and rotational motion can be obtained from the data, prior to LRI and then integrated into the reconstruction. Figure 4 shows equivalent traces alongside semi-quantitative metrics reconstructed with and without motion correction. Corresponding results from a constrained *in vivo* dictionary fit are in Figure 5. Though MTR and *f* are less affected, ihMTR and dipolar estimates are heavily artefacted before correction.

Discussion

Figure 3 demonstrates the effectiveness of our proposed framework since reconstructed signals show excellent agreement with results from a matched non-phase-encoded phantom experiment.

Figure 4 illustrates that retrospective motion estimation is successful for our *in vivo* dataset. Resultant ratio maps concur with the literature and previous simulations[3,4]: WM ihMTR~5-6%. The *in vivo* acquisition length was not optimal but ensured sufficient data was acquired. We expect scan time can be reduced to <30 minutes without significantly degrading image quality.

The reconstruction resolves temporal modulation of the signal, so it can be used for quantitative estimation as well as semi-quantitative MTR and ihMTR measurement. Cramér-Rao lower bound calculations indicated that 3-4 parameters can be simultaneously estimated using our current sequence. Since remaining parameters are fixed, bias may exist though fitted values largely agree with the literature: $T_{1D}{}^{s}$ is highest at 6.44±0.22ms in corticospinal tracts[11,12] but 2.79±0.12ms in GM, whereas f is highest at 0.111±0.006 in the corpus callosum[13] but 0.056±0.003 in GM.

Conclusion

We have presented a general method for transient fingerprinting-style scans in a motion corrected Cartesian framework. Further to the MT-based sequence shown here, this may prove a useful technique for high resolution MRF experiments using 3D acquisitions.

Acknowledgements

This work was supported by King's College London & Imperial College London EPSRC Centre for Doctoral Training in Medical Imaging [EP/L015226/1], by core funding from the Wellcome/EPSRC Centre for Medical Engineering [WT203148/Z/16/Z] and by the National Institute for Health Research (NIHR) Biomedical Research Centre based at Guy's and St Thomas' NHS Foundation Trust and King's College London and/or the NIHR Clinical Research Facility. The views expressed are those of the author(s) and not necessarily those of the NHS, the NIHR or the Department of Health and Social Care.

References

1. Girard, O. M. *et al.* Magnetization transfer from inhomogeneously broadened lines (ihMT): experimental optimization of saturation parameters for human brain imaging at 1.5 Tesla. *Magn. Reson. Med.* 73, 2111-2121 (2015).

2. Ercan, E. *et al.* Microstructural correlates of 3D steady-state inhomogeneous magnetization transfer (ihMT) in the human brain white matter assessed by myelin water imaging and diffusion tensor imaging. *Magn. Reson. Med.* 80, 2402-2414 (2018).

3. Malik, S. J., Teixeira, R. P. A. G., West, D. J., Wood, T. C. & Hajnal, J. V. Steady-state imaging with inhomogeneous magnetization transfer contrast using multiband radiofrequency pulses. *Magn. Reson. Med.* 83, 935-949 (2019).

4. West, D. J. *et al.* Transient-State Inhomogeneous Magnetisation Transfer: Towards Magnetisation Transfer Fingerprinting. *Proceedings of the 28th Annual Meeting of ISMRM* (2020).

5. West, D. J. *et al.* Magnetization Transfer-Mediated MR Fingerprinting. *Manuscript In Preparation.* (2020).

6. Assländer, J. *et al.* Low rank alternating direction method of multipliers reconstruction for MR fingerprinting. *Magn. Reson. Med.* 79, 83-96 (2018).

7. Cordero-Grande, L. *et al.* Sensitivity Encoding for Aligned Multishot Magnetic Resonance Reconstruction. *IEEE Trans. Comput. Imaging* 2, 266-280 (2016).

8. Cordero-Grande, L. *et al.* Motion corrected MRI with DISORDER: Distributed and Incoherent Sample Orders for Reconstruction Deblurring using Encoding Redundancy. *Magn. Reson. Med.* 84, 713-726 (2020).

9. Hilbert, T. *et al.* Magnetization Transfer in Magnetic Resonance Fingerprinting. *Magn. Reson. Med.* 84, 128-141 (2019).

10. Cohen, O., Huang, S., Mcmahon, M. T., Rosen, M. S. & Farrar, C. T. Rapid and quantitative chemical exchange saturation transfer (CEST) imaging with magnetic resonance fingerprinting (MRF). *Magn. Reson. Med.* 80, 2449-2463 (2018).

11. Swanson, S. D. *et al.* Molecular, dynamic and structural origin of inhomogeneous magnetization transfer in lipid membranes. *Magn. Reson. Med.* 77, 1318-1328 (2017).

12. Varma, G. *et al.* In vivo measurement of a new source of contrast, the dipolar relaxation time, T1D, using a modified inhomogeneous magnetization transfer (ihMT). sequence. *Magn. Reson. Med.* 78, 1362-1372 (2017).

13. Varma, G. *et al.* Low duty-cycle pulsed irradiation reduces magnetization transfer and increases the inhomogeneous magnetization transfer effect. *J. Magn. Reson.* 296, 60-71 (2018).

14. Mchinda, S. *et al.* Whole brain inhomogeneous magnetization transfer (ihMT) imaging: Sensitivity enhancement within a steady-state gradient echo sequence. *Magn. Reson. Med.* 79, 2607-2619 (2018).

Figures

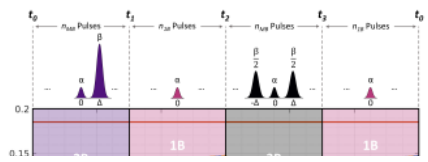

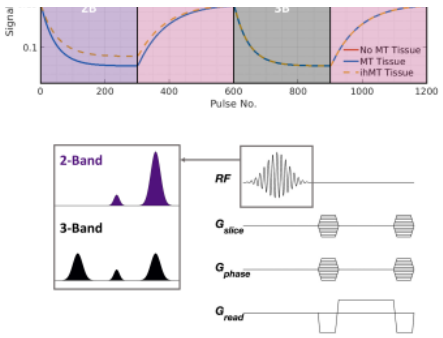

Figure 1: MT-MRF sequence structure. *Top*: Pulse alternation strategy and simulated tissue curves. *Bottom*: 1-band (1B), 2-band (2B) and 3-band (3B) pulses have identical on-resonance lobes (with power α) and are integrated into a balanced steady-state free precession (bSSFP) sequence module as shown (for multiband pulses only). The constant on-resonance flip angle means that "no MT" tissues give constant signal but signals from other tissues are strongly mediated by MT. MTR is calculated by comparing points t_2 and t_3, whilst ihMTR is calculated from points t_1 and t_3 normalized to t_2.

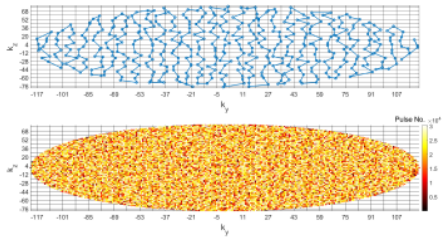

Figure 2: DISORDER *k*-space trajectory used in the phantom experiment. Each repetition comprises one pulse followed by a readout module where a single line of *k*-space is acquired. The phase-encoding plane was divided into 8-by-8 tiles (represented by grid lines); a pseudo-random *k*-space ordering was achieved by randomly sampling one position within each tile before moving to the next, proceeding in a zig-zag manner until all points were sampled. Distributed and randomized coverage of *k*-space enables motion estimation in flexible time windows and LRI respectively.

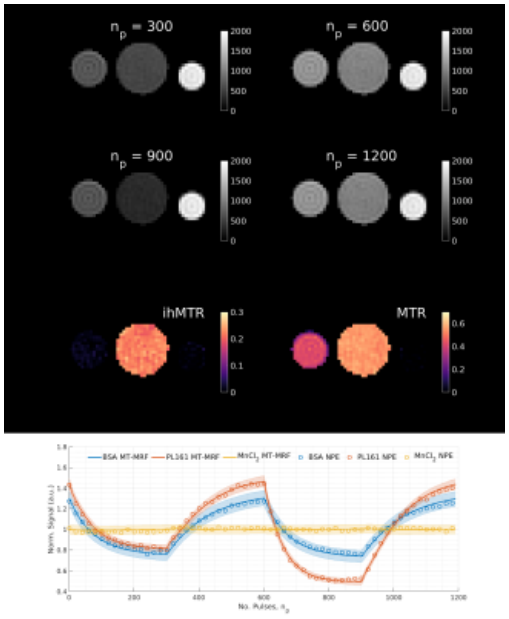

Figure 3: DISORDER phantom results. *Top*: Reconstructed images from one slice, shown for four different timepoints along the pulse cycle. *Middle*: MTR and ihMTR maps for the same slice produced using the above time domain images. *Bottom*: Reconstructed MT-MRF signal evolutions for a central region in each tube; excellent agreement is seen with respect to results from a corresponding non-phase-encoded (NPE) phantom experiment.

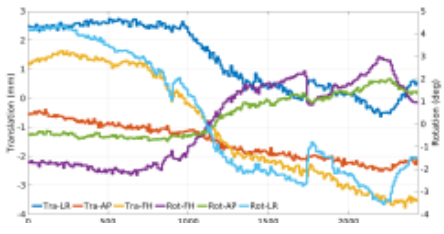

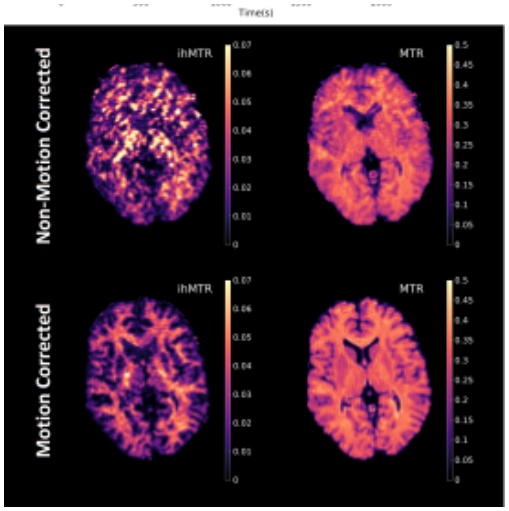

Figure 4: *Top*: Estimated motion traces during the *in vivo* acquisition. Results are from a compliant volunteer who was instructed not to move during the acquisition. "Tra" refers to transversal motion and "Rot" refers to rotation; "LR" indicates the left-right direction, "AP" is anterior-posterior, and "FH" is foot-head. *Bottom*: Example *in vivo* contrast ratio maps with and without motion correction from a central axial slice and reconstructed using the first eight singular components. MTR shows strong grey matter (GM)-white matter (WM) contrast and ihMTR is more correlated to WM.

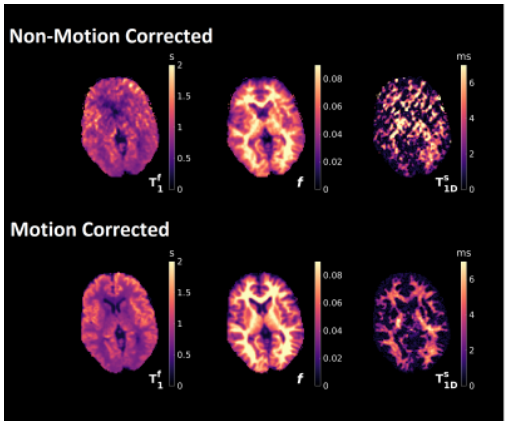

Figure 5: Dictionary fits to *in vivo* data with and without motion correction. Motion artefacts are significantly reduced for the former, enabling quantification of T_{1D}^s. The lower contrast-to-noise ratio of ihMT compared to MT means quantification of dipolar parameters is hindered prior to correction. GM-WM contrast appears enhanced for T_{1D}^s versus f and highly myelinated structures become more discernible. Semisolid relaxation times were fixed at T_{1Z}^s = 0.2s and T_2^s = 7.5μs; free pool T_2 at T_2^f = 69ms; exchange rate at K = 50s^{-1} and main magnetic field induced phase at ΔB_0 = 0[13,14].